STAR Protocols

CellPress
OPEN ACCESS

Protocol

Protocol on irradiation-dark photochemical deposition and characterization of metal nanoclusters on semiconductor support

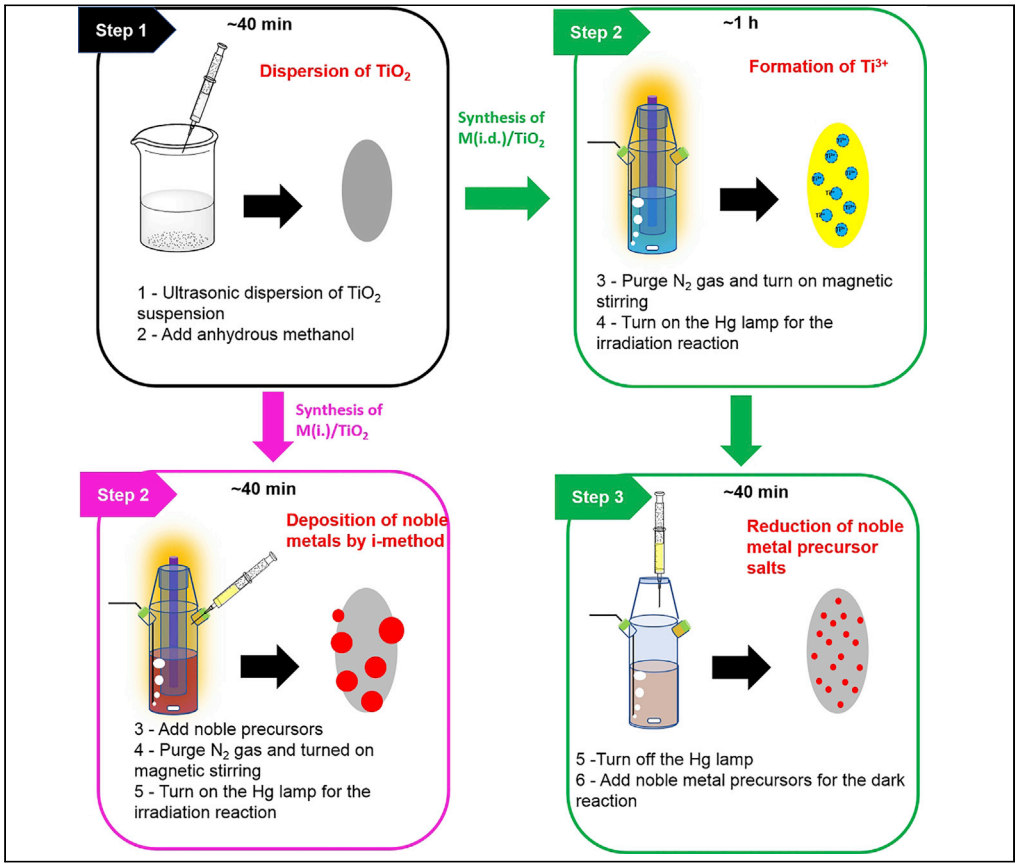

Controlling the size and uniform dispersion of noble metal nanoclusters on the metal oxide based semiconductor are difficult due to the natural tendency for metal atoms to agglomerate. Here, we present the protocol for an "irradiation-dark" photochemical deposition to obtain uniform metal nanoclusters on semiconductor support, λ and the protocol for measuring the size and size distribution of metal nanoclusters. For complete details on the use and execution of this protocol, please refer to (Wu et al., 2022).

Publisher's note: Undertaking any experimental protocol requires adherence to local institutional guidelines for laboratory safety and ethics.

Haocheng Wu, Yi Zhu, Rongrong Jia, Liyi Shi, Lei Huang

leihuang@shu.edu.cn

Highlights

Detailed protocol for the"irradiation-dark" photochemical deposition

Optimized approach for high loading amount

Characterization protocol of the size and size distribution of metal nanoclusters

Wu et al., STAR Protocols 3, 101459
September 16, 2022
https://doi.org/10.1016/j.xpro.2022.101459

STAR Protocols

CellPress
OPEN ACCESS

Protocol

Protocol on irradiation-dark photochemical deposition and characterization of metal nanoclusters on semiconductor support

Haocheng Wu,[1,3] Yi Zhu,[1,3] Rongrong Jia,[1] Liyi Shi,[1,2] and Lei Huang[1,4,5,*]

[1]Research Center of Nano Science and Technology, College of Sciences, Shanghai University, Shanghai 200444, P. R. China

[2]Emerging Industries Institute, Shanghai University, Jiaxing, Zhejiang 314006, P. R. China

[3]These authors contributed equally

[4]Technical contact

[5]Lead contact

*Correspondence: leihuang@shu.edu.cn
https://doi.org/10.1016/j.xpro.2022.101459

SUMMARY

Controlling the size and uniform dispersion of noble metal nanoclusters on the metal oxide based semiconductor are difficult due to the natural tendency for metal atoms to agglomerate. Here, we present the protocol for an "irradiation-dark" photochemical deposition to obtain uniform metal nanoclusters on semiconductor support, and the protocol for measuring the size and size distribution of metal nanoclusters. For complete details on the use and execution of this protocol, please refer to Wu et al. (2022).

BEFORE YOU BEGIN

The photodeposition method has demonstrated to be an effective strategy for the deposition of noble metals on semiconductor supports. However, traditional photodeposition easily forms Schottky junctions between metals and semiconductors, causing rapid electron transfer and resulting in uncontrollable growth rates and the preferred formation of large nanoparticles. In this work, an "irradiation-dark" (i.d.) process was developed to control the particle size. Different from the traditional "irradiation" (i.) method, firstly, Ti^{3+} is obtained as a charge storage form on the surface of TiO_2, and then the stored photogenerated electrons are used to reduce noble metal precursors in the dark, thereby controlling the nucleation and growth process of noble metal nanoparticles to gain uniform nanoclusters.

Preparation of metal precursor solutions

Timing: 30 min

1. Prepare a 0.01 g/mL $HAuCl_4 \cdot 4H_2O$ aqueous solution. Measure 1.0 g of $HAuCl_4 \cdot 4H_2O$ (Figure 1A), dilute with deionized water to 100 mL (Figure 1B).
2. Prepare a 0.01 g/mL $Pt(NH_3)_4(OH)_2 \cdot xH_2O$ aqueous solution. Measure 1.0 g of $Pt(NH_3)_4(OH)_2 \cdot xH_2O$, dilute with deionized water to 100 mL.
3. Prepare a 0.01 g/mL $PdCl_2$ aqueous solution. Measure 1.0 g of $PdCl_2$ and add 200 μL concentrated HCl (37%) and deionized water to dissolve, dilute it to 100 mL.
4. Prepare a 0.02 g/mL $AgNO_3$ aqueous solution. Measure 0.2 g of $AgNO_3$, dilute with deionized water to 10 mL. The corresponding devices are shown in Figure 1.
5. Store the prepared solutions at 4°C and must keep them in dark.

⚠ CRITICAL: Except the $AgNO_3$ aqueous solution which can only be used in 1 h, the other solutions can be stored for a week. $AgNO_3$ is easily photodegraded into Ag NPs in an

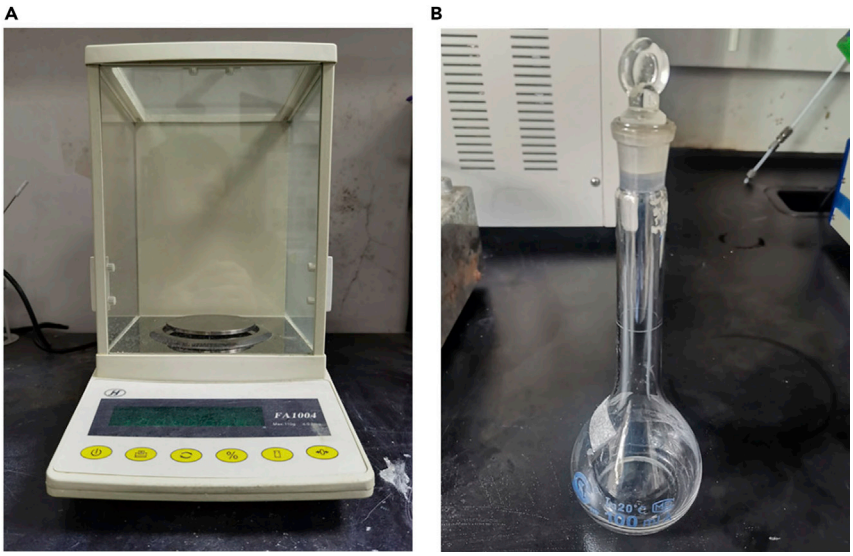

Figure 1. Equipment for precursor solutions preparation
(A) Electronic balance for weighing.
(B) Volumetric flask (100 mL) for dilution.

aqueous environment (Mahlman and Willmarth, 1964). In order to avoid the influence of photodegradation, all $AgNO_3$ aqueous solutions in this experiment must be prepared fresh before the experiments.

Preparation of equipment

Timing: 1.5 h

Preheat the photochemical reaction equipment.

6. Set the cooling water temperature to 13.5°C. Turn on the circulating cooling water pump (Figure 2D), and adjust the power of the lamp to 1000 W (Figure 2E).
7. Add 300 mL of deionized water and magnets to the 500 mL quartz photoreactor (Figure 2F). Turn on the Hg lamp (Figure 2H) and magnetic stirring (Figure 2C). Adjust the power to 1000 W (10 A × 100 V), start timing.
8. After the lamp stabilizes for 1 h, turn off the light source.
9. Prepare the N_2 generator (Figure 2A). Adjust the outlet pressure to 0.4 MPa. To ensure the purity of N_2 gas and control the O_2 concentration within 3 ppm, after turning on the gas generator, open the vent valve, and use it after venting for 30 min. N_2 gas cylinder (99.9 %) is also an option if the N_2 generator is unavailable.
10. Purge the deionized water in the quartz photoreactor with N_2. Adjust the N_2 flow rate to 40 mL/min through a flow meter.

⚠ CRITICAL: To ensure the purity of the gas produced by the gas generator, it is necessary to regularly check and replace the adsorbent in the filter device.

KEY RESOURCES TABLE

REAGENT or RESOURCE	SOURCE	IDENTIFIER
Chemicals, peptides, and recombinant proteins		
Zirconium dioxide (≥99.7% A.R.)	Macklin	CAS: 1314-23-4
Rutile titanium dioxide (≥99.5% C.P.)	Sigma-Aldrich	CAS: 1317-80-2

(*Continued on next page*)

Continued

REAGENT or RESOURCE	SOURCE	IDENTIFIER
Anatase titanium dioxide (≥99.7% A.R.)	Sigma-Aldrich	CAS: 1317-70-0
Tetraammineplatinum (II) hydroxide hydrate (≥99.5% C.P.)	Sigma-Aldrich	CAS: 15651-37-3
Chloroplatinic acid hexahydrate (≥99.7% A.R.)	Sinopharm	CAS: 18497-13-7
Chloroauric acid tetrahydrate (≥99.7% A.R.)	Sinopharm	CAS: 16903-35-8
Palladium chloride (≥99.7% A.R.)	Sinopharm	CAS: 7647-10-1
Silver nitrate (≥99.7% A.R.)	Sinopharm	CAS: 7761-88-8
Methanol (≥99.7% A.R.)	Sinopharm	CAS: 67-56-1
P25 titanium dioxide (≥99.5% C.P.)	JiangHuTaiBai	CAS: 13463-67-7
Hydrochloric acid (12 mol/L A.R.)	Sinopharm	CAS: 7647-01-0
Nitric acid (15.2 mol/L G.R.)	Sinopharm	CAS: 7697-37-2
Software and algorithms		
Origin 8.5	OriginLab	https://www.originlab.com/
MDI Jade 6	Materials Data Inc.	https://materialsdata.com/
Other		
Photochemical reaction equipment (Hg lamp, 1000 W)	Yuming	YM-GHX-I
N_2 generator	Zhonghuipu	NHA-300
Optical power meter	Thorlabs	PM100D
Ultrasonic cleaner	Chengxian	CX-500
Water-sealing vacuum pump	Chengxian	SHB-III
High-resolution transmission electron microscope (HRTEM)	JEOL	JEM-2010F and 2100F
X-ray powder diffractometer (XRD)	Rigaku	D/MAX2200V
UV-visible diffuse reflectance spectrometer (UV–Vis DRS)	Shimadzu	UV-2600
Electron paramagnetic resonance spectrometer (EPR)	Bruker	A300 EPR spectrometer
Inductively coupled plasma emission spectroscopy (ICP)	Jena	PQ-9000

MATERIALS AND EQUIPMENT

Alternative sources for reagents	
Reagent or resource	Alternate sources
Chemicals, peptides, and recombinant proteins	
Zirconium dioxide	Aladdin; Sigma-Aldrich
Rutile titanium dioxide	Aladdin
Anatase titanium dioxide	Aladdin
Tetraammineplatinum (II) hydroxide hydrate	Aladdin
Chloroplatinic acid hexahydrate	Aladdin; Sigma-Aldrich
Chloroauric acid tetrahydrate	Aladdin; Sigma-Aldrich
Palladium chloride	Aladdin; Sigma-Aldrich
Silver nitrate	Aladdin; Sigma-Aldrich
Methanol	Aladdin; Sigma-Aldrich; Macklin
Hydrochloric acid	Aladdin; Sigma-Aldrich
P25 titanium dioxide	Sigma-Aldrich

$HAuCl_4 \cdot 4H_2O$ aqueous solution		
Reagent	Final concentration concentrations	Volume to 100 mL
$HAuCl_4 \cdot 4H_2O$	0.01 g/mL	1.0 g
deionized water		100 mL
Store at 4°C. Use within 1 week.		

$Pt(NH_3)_4(OH)_2 \cdot xH_2O$ aqueous solution		
Reagent	Final concentration concentrations	Volume to 100 mL
$Pt(NH_3)_4(OH)_2 \cdot xH_2O$	0.01 g/mL	1.0 g
deionized water		100 mL
Store at 4°C. Use within 1 week.		

$PdCl_2$ aqueous solution		
Reagent	Final concentration concentrations	Volume to 100 mL
$PdCl_2$	0.01 g/mL	1.0 g
HCl (37%)		200 μL
deionized water		99.8 mL
Store at 4°C. Use within 1 week.		

$AgNO_3$ aqueous solution		
Reagent	Final concentration concentrations	Volume to 10 mL
$AgNO_3$	0.02 g/mL	0.2 g
deionized water		10 mL
Store at 4°C. Prepare within 1 h.		

STEP-BY-STEP METHOD DETAILS

Synthesis of M(i.)/TiO_2

Timing: 10.6 h

The samples prepared by the conventional photodeposition strategy were selected as the control group. In the presence of methanol (sacrificial reagent), the TiO_2 suspension to which the noble metal precursor salt was added was exposed to the irradiation of a Hg lamp. The photogenerated electrons transition to the surface of TiO_2 to reduce the metal precursor salt to form metal nanoparticles on TiO_2, and the photogenerated holes transition to the surface of TiO_2 to oxidize the sacrificial reagent (Haselmann et al., 2020; Meng et al., 2016; Wenderich and Mul, 2016).

1. Add 0.3 g TiO_2 powder to a beaker filled with 720 mL of deionized water, ultrasonically treat it for 30 min, and the ultrasonic power is 360 W.
2. Add 100 mL of anhydrous methanol and 10 mL diluted noble metal precursor salt aqueous solution such as $HAuCl_4 \cdot 4H_2O$ (1.57 mg/mL), $Pt(NH_3)_4(OH)_2 \, xH_2O$ (1.14 mg/mL), $AgNO_3$ (0.59 mg/mL), and $PdCl_2$ (1.25 mg/mL). Stir at 2000 r/min for 10 min.
3. Transfer the reaction solution to a quartz photoreactor, purge N_2 gas (40 mL/min), seal the reactor with rubber stoppers and parafilm.
4. Turn on the 1000 W Hg lamp (working wavelength as 365 nm) and adjust the intensity of the irradiation to 74 mW/cm^2, detected by an optical power meter (THORLABS PM100D).
5. The irradiation reaction was performed for 30 min at around 20°C.

⚠ CRITICAL: During the photoreaction process, keep the door of the reaction box closed. Do not look directly at the lamp. Wear optical protective glasses to avoid possible damage to the eyes when opening the door of the reaction box.

6. Separate the suspension through suction filtration with a 50 mm alcohol membrane with 0.45 μm aperture size to collect the solid precipitate.
7. Dry for 8 h at 60°C in the dark, and grind and collect the powders.

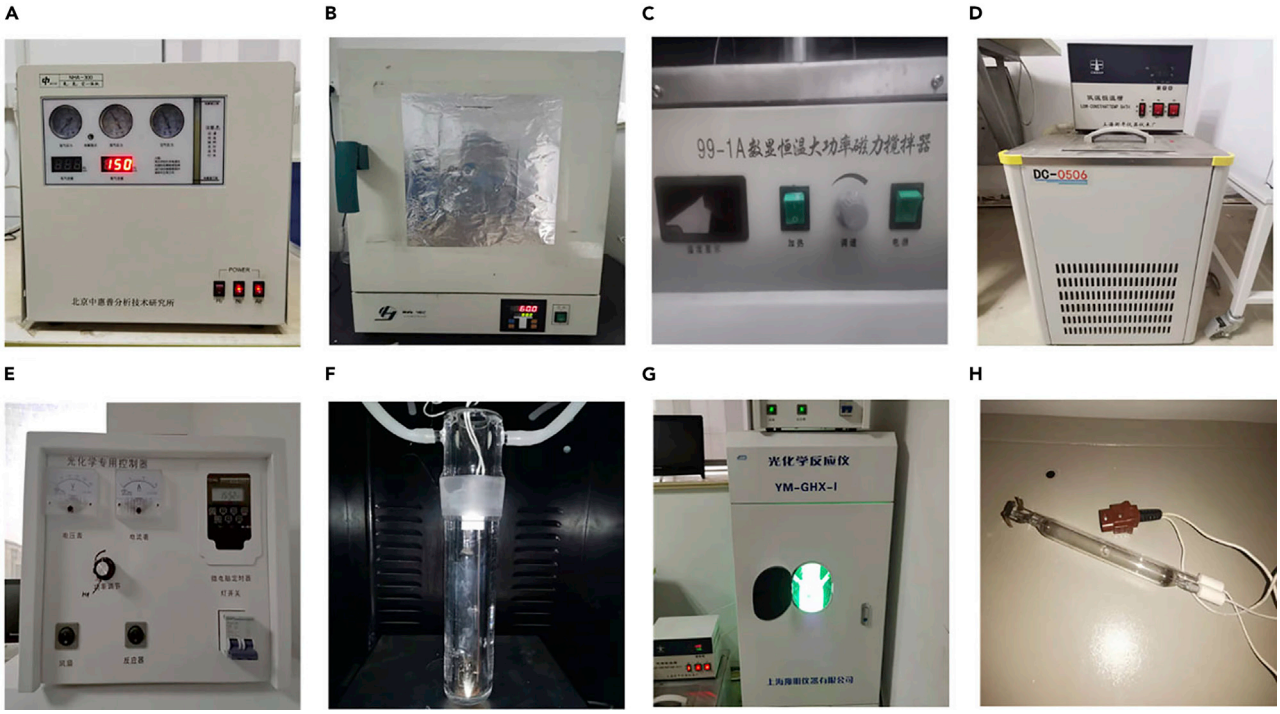

Figure 2. Photochemical reaction equipment for photodeposition

(A) N_2/H_2/Air gas generator.
(B) Dry oven.
(C) Magnetic stirrer.
(D) Circulating cooling pump.
(E) Power controller.
(F) Quartz jacket of the photoreactor.
(G) Reaction box.
(H) Mercury lamp.

8. The catalyst obtained by this method is labeled M(i.)/TiO_2(A/R), where (i.) means irradiation deposition, and A or R means that the crystal of TiO_2 is anatase or rutile.
9. Here, the loading amount of noble metals is 2.5 wt. %.

⚠ CRITICAL: After the precursor is added, the solution should be kept in the dark before the irradiation.

Synthesis of M(i.d.)/TiO_2

Timing: 9.5 h

In this work, an "irradiation-dark" (i.d.) process was developed to control the particle size. Different with the i. process, the TiO_2 suspension is containing methanol as sacrificial reagent was exposed to Hg lamp irradiation for 1 h. The TiO_2 was then reduced by the photoelectrons to get oxygen vacancy and Ti^{3+} species with the white TiO_2 suspension changes to blue. Turn off the light, noble metal precursor then is added and reduced by the Ti^{3+} species to form metal nanoclusters. The aqueous salt solution could be $HAuCl_4 \cdot 4H_2O$, Pt $(NH_3)_4(OH)_2$ xH_2O, $AgNO_3$, and $PdCl_2$.

10. Add 0.3 g of TiO_2 powder to 720 mL deionized water, ultrasonicate for 30 min with an ultrasonic power of 360 W, then add 100 mL of anhydrous methanol.
11. Irradiation reaction stage: transfer the TiO_2 suspension to the photoreactor.

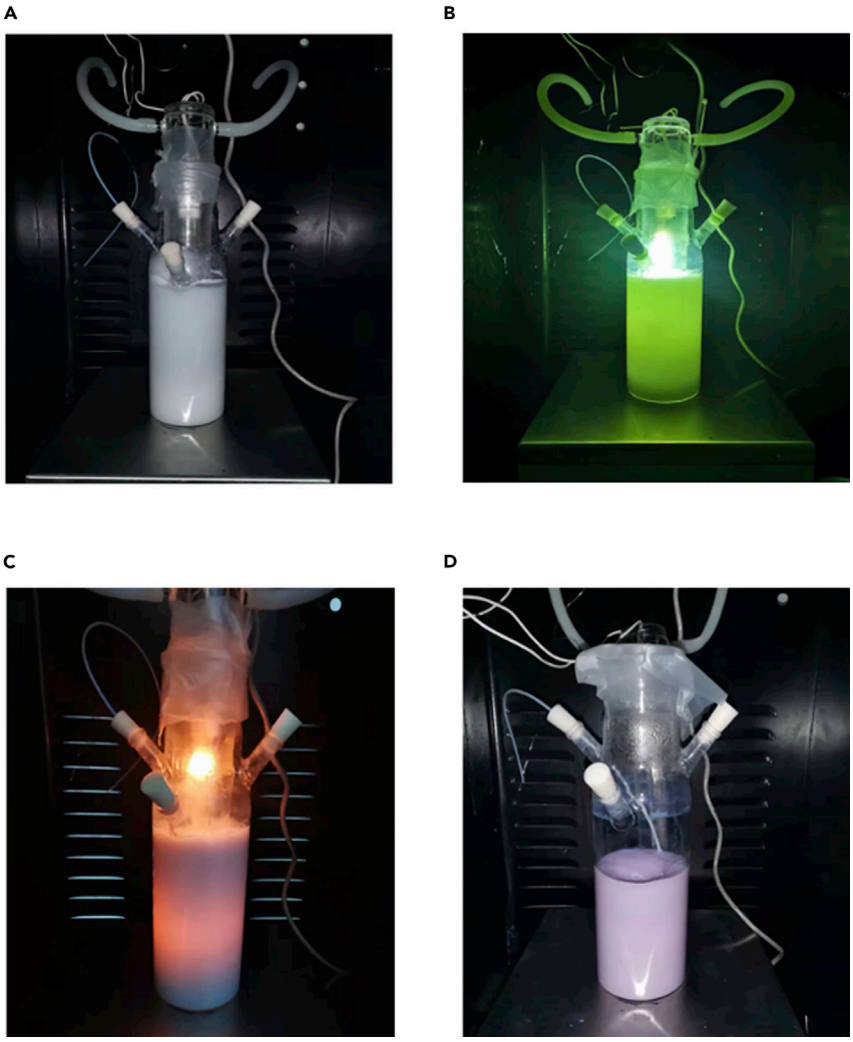

Figure 3. The photos of the photoreactor at different stages in the irradiation-dark (i.d.) photochemical deposition process

(A) Before photoreaction.
(B) During photoreaction.
(C) After photoreaction.
(D) After dark reaction.

12. Purge N_2 (40 mL/min) into the photoreactor and stir at 2000 r/min. Seal the reactor with rubber stoppers and parafilm. See Figure 3A.
13. Turn on the Hg lamp (74 mW/cm^2), and react in the irradiation for 30 min in the presence of circulating cooling water. See Figure 3B.
14. Dark reaction stage: turn off the light, take out the quartz jacket, keep stirring and maintain the N_2 flow.
15. Add 10 mL diluted noble metal precursor salt solution such as $HAuCl_4 \cdot 4H_2O$ (1.57 mg/mL), $Pt(NH_3)_4(OH)_2$ xH_2O (1.14 mg/mL), $AgNO_3$ (0.59 mg/mL), and $PdCl_2$ (1.25 mg/mL) to the reactor within 3 s with a 10 mL disposable dropper.
16. React for 30 min in the dark. See Figures 3C and 3D.
17. Separate the suspension through suction filtration. Collect the solid precipitate.
18. Dry for 8 h at 60°C in the dark, grind and collect the powders.
19. The catalyst obtained by this method is labeled M(i.d.)/TiO_2(A/R), where (i.d.) means irradiation-dark deposition, and A or R means that the crystal phase of TiO_2 is anatase or rutile.

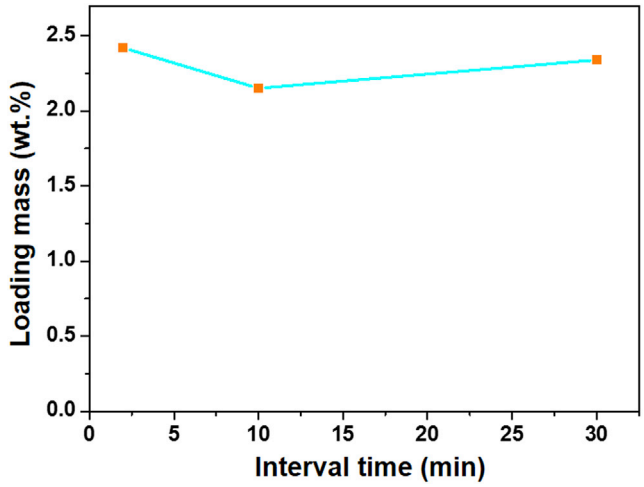

Figure 4. The loading amount of Au when Au(i.d.)/TiO_2(R) prepared at different injection intervals

⚠ CRITICAL: Be careful when moving out the quartz jacket since the Hg lamp is very hot. When the dropwise addition of the precursor solution is completed, the gap between the reactor and the light source liner is sealed again with a parafilm. The interval time (in 30 min) from the end of the irradiation to the addition of the metal precursor solution has negligible effect on the loading amount, as shown in Figure 4.

⚠ CRITICAL: The interval of adding the precursor solution after turning off the light is also used to deposit noble metals on other phases of TiO_2 (anatase and P25) and semiconductors (ZrO_2), and the experimental process is the same as M(i.d.)/TiO_2(R).

Structural characterization of M(i.)/TiO_2 and M(i.d.)/TiO_2

In order to characterize the size of noble metal particles deposited on TiO_2, high-resolution electron transmission microscope (HRTEM) and scanning transmission electron microscopy (STEM) are applied.

20. Take the sample powder (about 2.0 mg) into a 5.0 mL disposable sample tube.
21. Add 4 mL of absolute ethanol and sonicate for 20 min in a 360 W ultrasonic instrument.

⚠ CRITICAL: During the ultrasonic process, shake it vigorously to ensure that the powder is evenly dispersed in the alcohol solution. It is better that the final solution has weak optical rotation. The best ultrasound time is about 15–20 min. If the time is too short, the dispersion will not be good, which will affect the shooting process.

22. Copper mesh (Hengxin, HCF300-Cu) coated with ultra-thin carbon film is put on filter paper. Changing the specification from 300 item that we used to 200 item is also an alternative option. Cu should be changed to other metals such as Ni or Mo if the particles of copper itself are tested.
23. Use a disposable dropper to suck 7–8 drops of the suspension and add them to the copper mesh.
24. Put the copper mesh with the sample in the infrared rapid drying oven for 10 min, and then the HRTEM or the STEM test can be carried out.

Note: The samples can also be dried naturally.

25. Fix the prepared sample on the sample rod and insert it into the HRTEM (JEOL, JEM- 2010F and 2100F) microscope for testing. All tests are carried out at a high voltage of 200 kV.

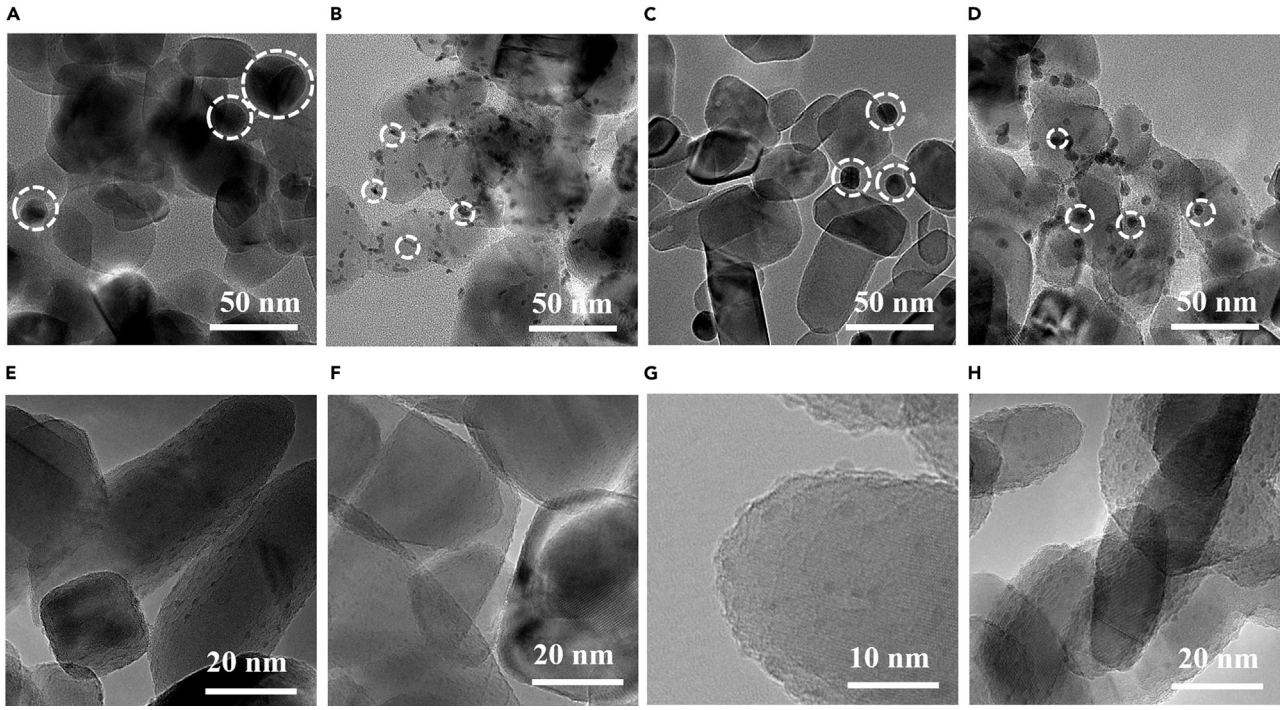

Figure 5. HRTEM images of different noble metals (Ag, Pt, Au and Pd) on TiO_2(R) by i. and i.d. method

(A) Ag(i.)/TiO_2(R).
(B) Pt(i.)/TiO_2(R).
(C) Au(i.)/TiO_2(R).
(D) Pd(i.)/TiO_2(R).
(E) Ag(i.d.)/TiO_2(R).
(F) Pt(i.d.)/TiO_2(R).
(G) Au(i.d.)/TiO_2(R).
(H) Pd(i.d.)/TiO_2(R).

26. Analyze the size of metals and supports according to the HRTEM images. We can distinguish noble metals and the support by contrast, the ones with large contrast are noble metals, and those with small contrast are titanium oxides.
27. Analyze the M(i.)/TiO_2(R).
    a. The average particle size of Au, Ag, Pt, Pd supported on TiO_2(R) are 12.8 nm, 11.1 nm, 3.4 nm and 3.2 nm, respectively (Wu et al., 2022).The particles are large and the agglomeration is apparent (Figures 5A–5D).
    b. According to the HRTEM images of M(i.d.)/TiO_2(R): The average particle size of Au, Ag, Pt, Pd supported on TiO_2(R) are 0.6 nm, 0.5 nm, 0.5 nm and 0.7 nm, respectively (Wu et al., 2022). The particles are smaller, and the size is well controlled (Figures 5E–5H).
28. STEM can also demonstrate the deposition of noble metal particles, showing in Figure 6.

XRD is used to analyze the crystal structure of materials (Lupescu et al., 2018). By analyzing the peaks, the size of noble metals supported on TiO_2 can be explored.

29. Take 0.2 g of the prepared sample and spread it in the 1 cm × 1 cm groove of the quartz sample table, flatten the surface with a glass sheet and carry out testing.
30. Increase the voltage of the device (D/MAX2200V) to 40 kV and the current to 40 mA. The scanning range is 30°-50° (It can be adjusted depending on different metals), and the scanning speed is 10 °/min.

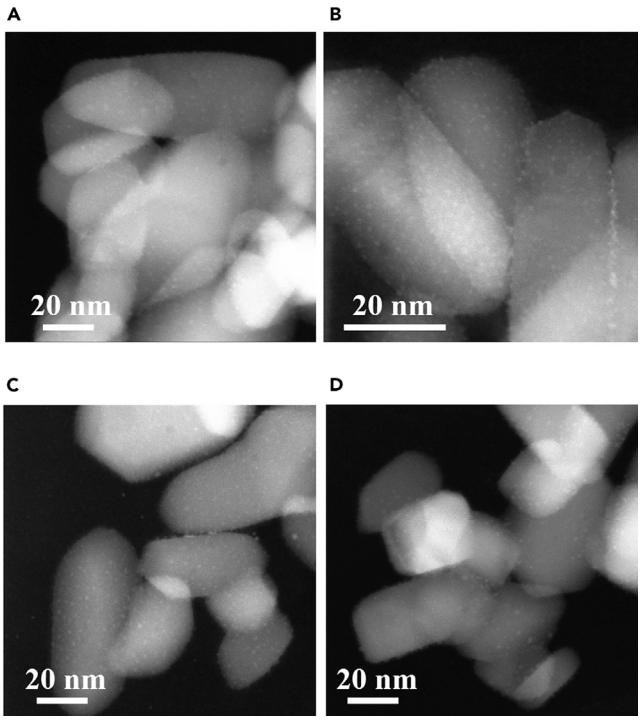

Figure 6. STEM images of different noble metals (Ag, Pt, Au and Pd) on TiO_2(R) by i.d. method

(A) Ag(i.d.)/TiO_2(R).

(B) Pt(i.d.)/TiO_2(R).

(C) Au(i.d.)/TiO_2(R).

(D) Pd(i.d.)/TiO_2(R).

31. The crystal phase can be identified by three major XRD diffraction peaks. All samples have rutile diffraction peaks at 2 θ of 36°, 39.2°, 41.2° and 44.05°, which proves that the support is rutile (Holm et al., 2019).
32. Besides TiO_2 peaks, look for corresponding noble metal peaks in XRD for both M(i.)/TiO_2(R) and M(i.d.)/TiO_2(R) (Figure 7). Take Figure 7A for an example, a diffraction peak corresponding to Ag can be seen at 38.1° for Ag(i.)/TiO_2(R), but it can hardly be seen for Ag(i.d.)/TiO_2(R).
33. Analyze the size of noble metals based on the XRD patterns. The larger the size of the metal particles is, the higher the peaks intensity will be.

⚠ CRITICAL: High intensity indicates that the size of the particles by the i. method is larger than the i.d. method, and those deposited by the i.d. method are well controlled.

UV-vis DRS is a classical method to characterize the optical properties of materials. Especially for noble metals with localized surface plasmon resonance (LSPR) effect, such as Au and Ag, it is a conventional method to reveal the change of particle size (Forcherio and Roper, 2016).

34. Set the slit of the instrument as 1 nm. The $BaSO_4$ integrating sphere is used for background correction. The test scanning wavelength range is 200–800 nm, and the scanning speed is 480 nm/min.
35. Take 0.25 g of the prepared powder into the sample cell and slowly tighten the back cover to make the powder evenly and tightly spread under the quartz glass for testing.

⚠ CRITICAL: The sample must be evenly spread over the entire quartz glass. Otherwise, it will affect the accuracy.

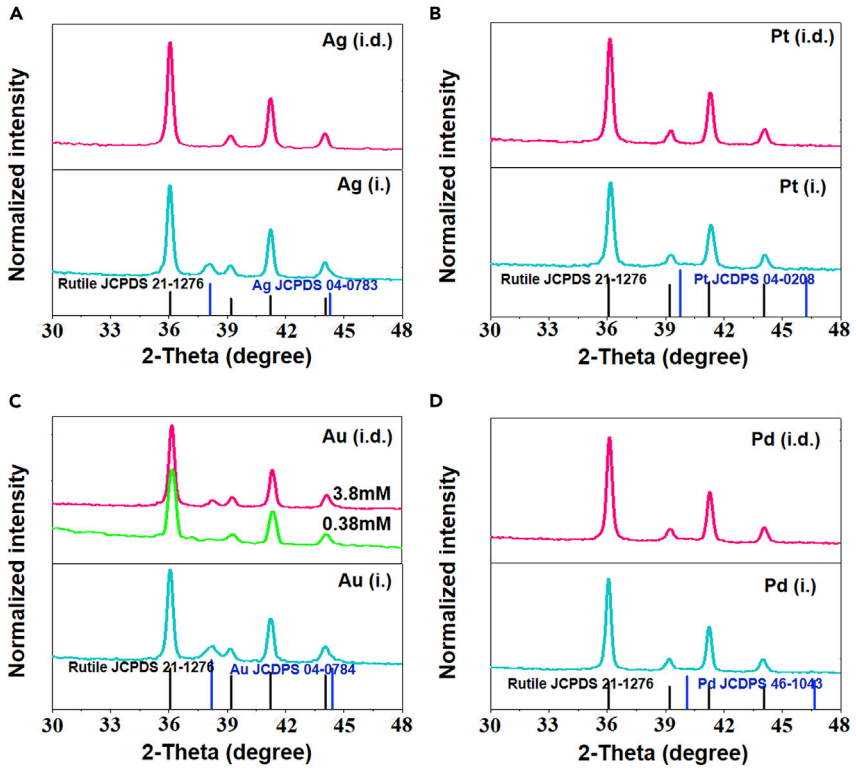

Figure 7. XRD patterns of different samples

(A) XRD patterns of Ag/TiO_2(R).

(B) XRD patterns of Pt/TiO_2(R).

(C) XRD patterns of Au/TiO_2(R). 3.8 mM is the concentration of $HAuCl_4$ aqueous solution with a volume of 10 mL and 0.38 mM corresponds to the concentration of 100 mL aqueous solution, accordingly.

(D) XRD patterns of Pd/TiO_2(R). Figure reprinted with permission from (Wu et al., 2022).

36. The characteristic absorption peaks of Au and Ag are 550 nm (Dulnee et al., 2014) and 470 nm (Wu et al., 2020) in Au(i.)/TiO_2(R) and Ag(i.)/TiO_2(R). By identifying the high peaks of characteristic absorption, it indicates that the noble metal particles deposited by the method i. are larger in size. See Figure 8.
37. The absorption peak intensity of M(i.d.)/TiO_2(R) is weak. The characteristic absorption peaks of Au and Ag located at 550 nm and 470 nm in Au(i.)/TiO_2(R) and Ag(i.)/TiO_2(R) are not detected, indicating that the size of the noble metal particles deposited by the i.d. method is small.

In order to explore the loading amount at different dark reaction intervals and the final content of noble metals deposited by the i.d. method, an inductive coupled plasma emission spectrometer (ICP) was used for testing.

38. Before testing, dilute the noble metal standard solution (Beijing Nonferrous Metals Research Institute, the original standard solution of Au, Pt, Pd: 10 mg/mL; Ag: 1 mg/mL) with 2% dilute nitric acid solution to 0.1, 0.3, 0.5, 0.7, 1.0 mg/mL, test by ICP and draw the standard curve.
39. For detecting the loading amount of metals on TiO_2, the reaction suspension at different dark reaction intervals is filtered using a syringe membrane filter with a pore size of 0.22 μm to obtain a clear filtrate.
40. Take 1 mL of filtrate, add 8.8 mL of deionized water and 200 μL of concentrated nitric acid (GR) to obtain a 2% dilute nitric acid test solution for ICP test.
41. All samples are tested 3 times and take the average value.

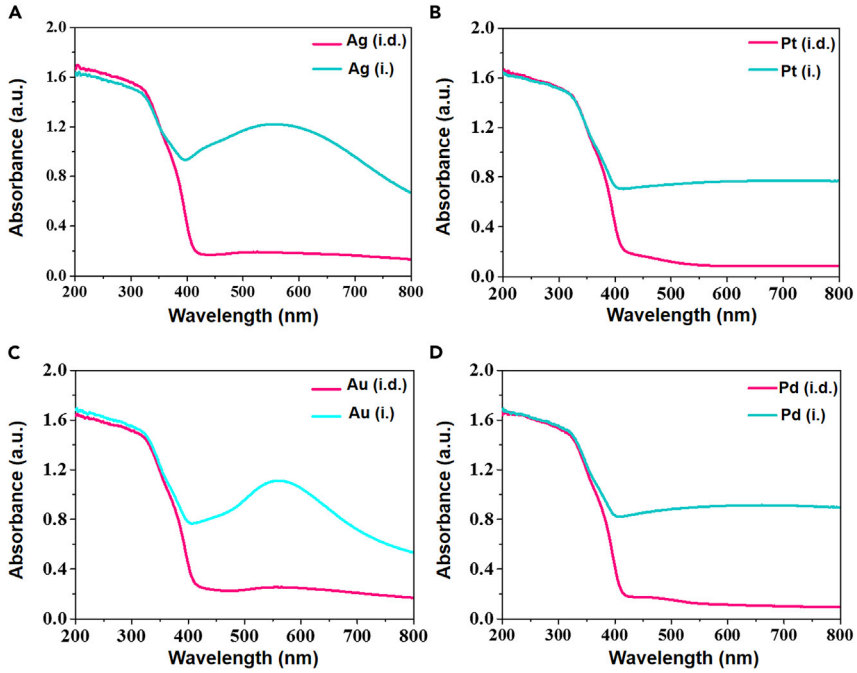

Figure 8. UV–Vis DRS spectra of M/TiO_2(R) by i. and i.d. methods

(A) Ag/TiO_2(R).

(B) Pt/TiO_2(R).

(C) Au/TiO_2(R).

(D) Pd/TiO_2(R). Figure reprinted with permission from (Wu et al., 2022).

⚠ CRITICAL: The powders need to be fully separated from the suspension to avoid blocking the equipment and make the result accurate. The charge of the metal precursors has a significant influence on the loading amount. For the negatively charged $AuCl_4^-$, the actual loading is close to the loading amount, while for the positively charged $Pt(NH_3)_4^{2+}$, Pd^{2+}, Ag^+, the actual loading is all lower than the designed loading amount. See Table 1. Therefore, it's important to choose the charges of TiO_2 and the metal precursors.

Experiments under different conditions

42. HRTEM, XRD and UV-vis DRS: Replace the carrier with different metal oxide supports such as anatase TiO_2, P25 TiO_2 and ZrO_2 (Wu et al., 2022).
43. UV-vis DRS experiment with different light intensity: In order to study the difference in metal deposition kinetics caused by light intensity, the light intensity was reduced from 74 mW/cm^2 to 12 and 2 mW/cm^2 for photodeposition (Wu et al., 2022).

EXPECTED OUTCOMES

In this protocol, the deposition process of metal nanoclusters on semiconductor support through an "irradiation-dark" process was present. Different noble metal nanoclusters, including Au, Ag, Pd, Pd, could be successfully loaded on semiconductors. The uniform size could be controlled smaller than 1.0 nm. We also demonstrated the promoted performance in the catalytic oxidation of HCHO over Pt and Au nanocluster on TiO_2 (Wu et al., 2022). We believe the combinations of different metal-supports could be used as effective catalysts in other heterogeneous catalysis.

LIMITATIONS

According to the proposed strategies, the photoelectrons are firstly stored as Ti^{3+}, then released to reduce the metal precursors in the dark. It requires the semiconductor support enables to store

Table 1. Comparison of the designed loading capacities of noble metals and the loading amount estimated by ICP

Sample	Metal precursor	Noble metals	Photodeposition condition	Nominal M[a] (wt. %)	Measured M[a] by ICP-OES (wt. %)
Au(i.d.)/TiO_2(R)	$AuCl_4^-$	Au	0.5 h dark after Hg lamp (74 mW/cm^2),1.0 h	2.5	2.43 ± 0.05[b]
Pt(i.d.)/TiO_2(R)	$PtCl_6^{2-}$	Pt	0.5 h dark after Hg lamp (74 mW/cm^2),1.0 h	2.5	2.39 ± 0.04 [b]
Ag(i.d.)/TiO_2(R)	Ag^+	Ag	0.5 h dark after Hg lamp (74 mW/cm^2),1.0 h	2.5	0.49 ± 0.08 [b]
Pd(i.d.)/TiO_2(R)	Pd^{2+}	Pd	0.5 h dark after Hg lamp (74 mW/cm^2),1.0 h	2.5	0.18 ± 0.01 [b]
Pt(i.d.)/TiO_2(R)	$[Pt(NH_3)_4]^{2+}$	Pt	0.5 h dark after Hg lamp (74 mW/cm^2),1.0 h	2.5	0.80 ± 0.02 [b]
Pt(i.d.)/TiO_2(R)	$PtCl_6^{2-}$	Pt	0.5 h dark after Hg lamp (74 mW/cm^2),.3.0 h	2.5	2.49 ± 0.01
Pt(i.d.)/TiO_2(R)	$PtCl_6^{2-}$	Pt	0.5 h dark after Hg lamp (74 mW/cm^2),1.0 h	10.0	6.25 ± 0.06
Pt(i.d.)/TiO_2(R)	$PtCl_6^{2-}$	Pt	0.5 h dark after Hg lamp (74 mW/cm^2),3.0 h	10.0	9.96 ± 0.04

[a]M=Au、Ag、Pt、Pd.
[b]indicates that the data is from (Wu et al., 2022).

photogenerated charges via a redox process . Besides, the reduced species should be thermodynamically favorable for the reduction of noble metal precursors. Therefore, not all the semiconductor supports are applicable.

TROUBLESHOOTING

Problem 1

Different metal precursors have different concentrations during the dark reaction. If the deposition rate and concentration do not match, it may lead to the formation of larger nanoparticles. For example, when Au(i.d.)/TiO_2(R) is prepared by the above method, a small amount of Au nanoparticles is larger in size, and diffraction peaks can be clearly observed in XRD shown in Figure 7C.

Potential solution

Reduce the concentration of the metal precursor solution to avoid the formation of large nanoparticles due to the high local concentration of metal ions., keeping the molar mass of the metal precursor salt unchanged. For example, if the precursor solution of $HAuCl_4 \cdot 4H_2O$ is diluted from 1.57 mg/mL (3.8 mM) to 0.157 mg/mL (0.38 mM), the bigger sizes of Au nanoparticles are highly reduced as confirmed by the disappearance of the diffraction peak of Au in XRD shown in Figure 7C. (Synthesis of M(i.d.)/TiO_2 step 15).

Problem 2

When the charge of the metal precursor salt and the TiO_2 surface are contrary, the metal loading may be reduced. For example, when chloroplatinic acid is used to prepare Pt(i.d.)/TiO_2(R), the supporting amount of Pt is relatively low. The designed supporting amount is 2.5 wt. %, but only 0.8 wt. % of Pt is successfully loaded.

Potential solution

Replace the charging performance of the precursor salt. For example, replacing the negatively charged $H_2PtCl_6 \cdot 6H_2O$ with the positively charged $Pt(NH_3)_4(OH)_2 \cdot xH_2O$ can increase the Pt loading from the previous 0.8 wt. % to 2.4 wt. % (Table 1).

Problem 3

In the dark reaction stage, the method of directly pouring the noble metal precursor liquid cannot ensure the maximum liquid-liquid mass transfer, resulting in the formation of large nanoparticles.

Potential solution

A 10 mL disposable dropper is used to add the precursor liquid at the center of the liquid vortex to enhance the mass transfer and avoid the formation of large particles. (Synthesis of M(i.)/TiO_2 step 2).

Problem 4

Practical industrial production requires high load catalysts (Yoo et al., 2020). Thus promoting the loading amounts of metals is an important problem to solve.

Potential solution

Extend the time of the photoreaction thus increase the amount of Ti^{3+}, so as to obtain a higher loading amount of noble metal nanoclusters. For example, by extending the photoreaction time from 1 h to 3 h, the loading amount of Pt can be promoted from 6.25 wt. % to about 10 wt. % at the designed loading of 10 wt. % (Table 1).

Problem 5

The N_2 flow rate in the photoreaction stage should not be too high. If the flow rate is too high, the support will hang on the inner wall of the reactor and affect the reaction process.

Potential solution

Adjust the flow rate before reaction carefully. We set the N_2 flow rate to 40 mL/min through a flow meter to avoid this situation. (Synthesis of M(i.d.)/TiO_2 step 13).

RESOURCE AVAILABILITY

Lead contact

Further information and requests for resources and reagents should be directed to and will be fulfilled by the lead contact, Lei Huang (leihuang@shu.edu.cn).

Materials availability

This study did not generate new unique reagents.

Data and code availability

All data reported in this paper will be shared by the lead contact upon request.

This paper does not report original code.

Any additional information required to analyze the data reported in this paper is available from the lead contact upon request.

ACKNOWLEDGMENTS

This work is financially supported by Shanghai Municipal Science and Technology Commission (18520744500, 19DZ2293100, 21DZ2280600).

AUTHOR CONTRIBUTIONS

L.H. directed and conceived this work. H.C.W. and Y.Z. performed the photodeposition experiments and analyzed the data. R.R.J. participated in the discussion of experiments and commented on the draft. L.Y.S. provided funding, supporting, project administration, and supervision of the experiments. L.H., Y.Z., and H.C.W. wrote the manuscript with edits and approval from all authors.

DECLARATION OF INTERESTS

The authors declare no competing interests.

REFERENCES

Dulnee, S., Luengnaruemitchai, A., and Wanchanthuek, R. (2014). Activity of Au/ZnO catalysts prepared by photodeposition for the preferential CO oxidation in a H_2-rich gas. Int. J. Hydrog. Energy *39*, 6443–6453. https://doi.org/10.1016/j.ijhydene.2014.02.038.

Forcherio, G.T., and Roper, D.K. (2016). Spectral characteristics of noble metal nanoparticle-molybdenum disulfide heterostructures. Adv. Opt. Mater. *4*, 1288–1294. https://doi.org/10.1002/adom.201600219.

Haselmann, G.M., Baumgartner, B., Wang, J., Wieland, K., Gupta, T., Herzig, C., Limbeck, A., Lendl, B., and Eder, D. (2020). In situ Pt photodeposition and methanol photooxidation on Pt/TiO_2: Pt-loading-dependent photocatalytic reaction pathways studied by liquid-phase infrared spectroscopy. ACS Catal. *10*, 2964–2977. https://doi.org/10.1021/acscatal.9b05588.

Holm, A., Hamandi, M., Simonet, F., Jouguet, B., Dappozze, F., and Guillard, C. (2019). Impact of rutile and anatase phase on the photocatalytic decomposition of lactic acid. Appl. Catal. B Environ. *253*, 96–104. https://doi.org/10.1016/j.apcatb.2019.04.042.

Lupescu, J.A., Schwank, J.W., Fisher, G.B., Hangas, J., Peczonczyk, S.L., and Paxton, W.A. (2018). Pd model catalysts: effect of air pulse length during redox aging on Pd redispersion. Appl. Catal. B Environ. *223*, 76–90. https://doi.org/10.1016/j.apcatb.2017.07.055.

Mahlman, H.A., and Willmarth, T.E. (1964). Radiolytic and photolytic reduction of aqueous silver nitrate solutions. Nature *202*, 590–591. https://doi.org/10.1038/202590a0.

Meng, A., Zhang, J., Xu, D., Cheng, B., and Yu, J. (2016). Enhanced photocatalytic H_2 production activity of anatase TiO_2 nanosheet by selectively depositing dual-cocatalysts on {101} and {001} facets. Appl. Catal. B Environ. *198*, 286–294. https://doi.org/10.1016/j.apcatb.2016.05.074.

Wenderich, K., and Mul, G. (2016). Methods, mechanism, and applications of photodeposition in photocatalysis: a review. Chem. Rev. *116*, 14587–14619. https://doi.org/10.1021/acs.chemrev.6b00327.

Wu, H., Jiang, W., Shi, L., Li, R., Huang, L., and Li, C. (2022). Photo-assisted sequential assembling of uniform metal nanoclusters on semiconductor support. iScience *25*, 103572. https://doi.org/10.1016/j.isci.2021.103572.

Wu, J.D., Wang, Y.Q., Liu, Z.X., Yan, Y.S., and Zhu, Z. (2020). Preparation of noble metal Ag-modified $BiVO_4$ nanosheets and a study on the degradation performance of tetracyclines. New J. Chem. *44*, 13815–13823. https://doi.org/10.1039/d0nj03080e.

Yoo, T.Y., Yoo, J.M., Sinha, A.K., Bootharaju, M.S., Jung, E., Lee, H.S., Lee, B.-H., Kim, J., Antink, W.H., Kim, Y.M., et al. (2020). Direct synthesis of intermetallic platinum-alloy nanoparticles highly loaded on carbon supports for efficient electrocatalysis. J. Am. Chem. Soc. *142*, 14190–14200. https://doi.org/10.1021/jacs.0c05140.